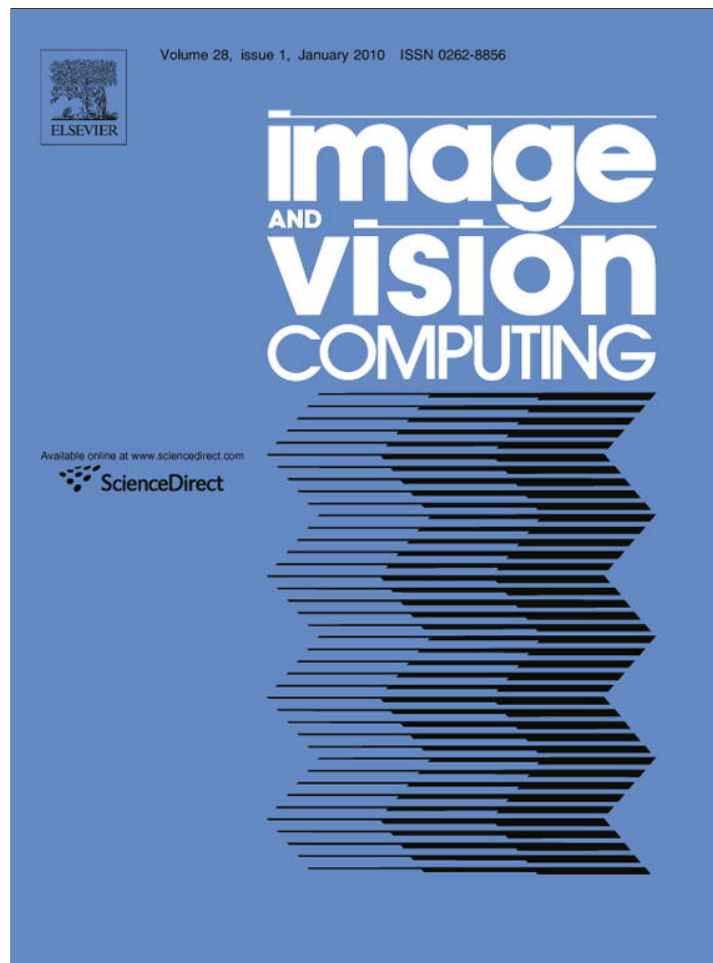


Provided for non-commercial research and education use.  
Not for reproduction, distribution or commercial use.



This article appeared in a journal published by Elsevier. The attached copy is furnished to the author for internal non-commercial research and education use, including for instruction at the authors institution and sharing with colleagues.

Other uses, including reproduction and distribution, or selling or licensing copies, or posting to personal, institutional or third party websites are prohibited.

In most cases authors are permitted to post their version of the article (e.g. in Word or Tex form) to their personal website or institutional repository. Authors requiring further information regarding Elsevier's archiving and manuscript policies are encouraged to visit:

<http://www.elsevier.com/copyright>



Contents lists available at ScienceDirect

## Image and Vision Computing

journal homepage: [www.elsevier.com/locate/imavis](http://www.elsevier.com/locate/imavis)

Short communication

## Iris recognition: Analysis of the error rates regarding the accuracy of the segmentation stage

Hugo Proença\*, Luís A. Alexandre

University of Beira Interior, Department of Computer Science, IT – Institute of Telecommunications, Networks and Multimedia Group, 6200 Covilhã, Portugal

## ARTICLE INFO

## Article history:

Received 9 December 2006

Received in revised form 25 November 2008

Accepted 5 March 2009

## Keywords:

Biometrics

Image segmentation

Iris recognition

## ABSTRACT

Iris recognition has been widely used in several scenarios with very satisfactory results. As it is one of the earliest stages, the image segmentation is in the basis of the process and plays a crucial role in the success of the recognition task. In this paper we analyze the relationship between the accuracy of the iris segmentation process and the error rates of three typical iris recognition methods. We selected 5000 images of the UBIRIS, CASIA and ICE databases that the used segmentation algorithm can accurately segment and artificially simulated four types of segmentation inaccuracies. The obtained results allowed us to conclude about a strong relationship between translational segmentation inaccuracies – that lead to errors in phase – and the recognition error rates.

© 2009 Elsevier B.V. All rights reserved.

## 1. Introduction

The use of biometric systems has been increasingly encouraged by both government and private entities, in order to replace or improve traditional security systems. The iris is recognized as one of the most reliable biometric traits: it has a random morphogenesis and high complexity, making individual patterns apparently unique.

Using inflexible image capturing conditions and protocols it is possible to acquire images with good quality and achieve impressive accuracy, with very low error rates. Also, most of the failure cases (usually false non-matches) occur when images do not have enough quality, either due to focus, contrast or brightness problems resultant of improper lighting or due to iris occlusions by eyelids, eyelashes, glasses, contact lenses or reflections. This problem was identified by several authors (e.g., [1–3]) and concerns a growing number of researchers.

Regarding an iris recognition system as an image processing task, the role of the segmentation stage in the final results can be easily anticipated. As it is usually the earliest stage, any failure compromises the whole process. Also, it is the stage that more directly should handle the raw data's heterogeneity, resultant of non-ideal imaging. Independently of the accuracy of the used segmentation methods, it is realistic to consider that dynamic lighting conditions and less constrained imaging protocols should lead to the existence of segmentation inaccuracies, i.e., small errors between the detected and the true iris borders.

In this paper our goal consists in the analysis of the relationship between the accuracy of the segmentation process and the error

rates of typical recognition systems. In order to achieve this, we performed the following experimental procedure:

- (1) Selection of 5000 images of the UBIRIS (first [4] and second [17] versions), CASIA (third version [5]) and ICE [6] databases. Manual verification that the used iris segmentation algorithm is able to accurately segment all the images.
- (2) Feature extraction on accurately segmented images: extraction of the biometric iris signatures according to three distinct iris encoding strategies that we believe to represent the most usual approaches.
- (3) Feature comparison: comparison, using the Hamming distance, between the iris signatures extracted in the previous stage.
- (4) Simulation of segmentation inaccuracies. Corruption of the segmentation algorithm in order to less accurately localize the iris borders.
- (5) Feature extraction and comparison on inaccurately segmented images: extraction and comparison of the resulting signatures through the previously used methods.

It should be stressed that this analysis is independent of the choice of the segmentation algorithm, as we manually verified that the used one is able to accurately localize both iris borders (pupillary and scleric) of all the used images. Oppositely, it is dependent of the three used feature extraction methods [8,9,2]. These were selected respectively due to their relevance in the literature [8] and to the fact of share the use of normalized and pseudo-polar images to extract binary iris signatures [9,2].

The remaining sections of this paper are organized as follows: Section 2 briefly summarizes the most cited iris recognition meth-

\* Corresponding author. Tel.: +351 961855361.

E-mail addresses: [hugomcp@di.ubi.pt](mailto:hugomcp@di.ubi.pt) (H. Proença), [lfaa@di.ubi.pt](mailto:lfaa@di.ubi.pt) (L.A. Alexandre).

ods and overviews some of the most relevant iris segmentation approaches. Section 3 analyzes and discusses the influence of each type of segmentation error in the recognition accuracy and, finally, Section 5 gives the conclusions.

## 2. Iris recognition

Fig. 1 gives a block diagram that contains the typical stages of the published iris recognition methods. In spite of the specificities of each proposal, the large majority share the given structure.

The initial stage concerns about the segmentation of the iris. This consists in localize the iris inner (pupillary) and outer (scleric) boundaries, assuming either circular or elliptical shapes for each border. Additionally, it is usual to detect regions of the iris texture occluded by any other type of data, as eyelids, eyelashes, glasses or hair.

In order to compensate variations in the pupils sizes and in the image capturing distances, the segmented data is translated into a fixed length and dimensionless polar coordinate system, which is usually performed through the method proposed by Daugman [8].

Regarding feature extraction, iris recognition approaches can be divided into three major categories: phase-based methods (e.g., Daugman [8]), zero-crossing methods (e.g., Boles and Boashash [10]) and texture-analysis based methods (e.g., Wildes [1]). Daugman [8] used multi-scale quadrature wavelets to extract phase information from the iris texture and obtain a biometric signature with 2048 binary components. Boles and Boashash [10] computed the zero-crossing representation of an unidimensional wavelet at different scales of concentric circles and Wildes [1] proposed the characterization of the iris texture through a Laplacian pyramid with four different levels (scales).

On the final stage it is performed a comparison between iris signatures, yielding a numeric dissimilarity value. If this is higher than a threshold, the system outputs a *non-match*, meaning that each signature belongs to different irises. Otherwise, the system outputs a *match*, meaning that both signatures were extracted from images of the same iris.

As the schema of Fig. 1 illustrates, the segmentation stage is in the basis of the process, which explains its major role. In the next sub-section we overview some of the most relevant approaches to perform the segmentation of the iris on close-up iris images.

### 2.1. Iris segmentation methods

There are two major strategies to perform the segmentation of the iris: use a rigid or deformable iris template or use its boundary. In most cases, the boundary-based approach starts by the construction of an edge-map, followed by the application of some geometric form fitting method. Template-based strategies usually include the maximization of some equation and are in general more heterogeneous.

In 1993, Daugman [7] published one of the most cited methods, which was used on near all the commercially deployed systems. He

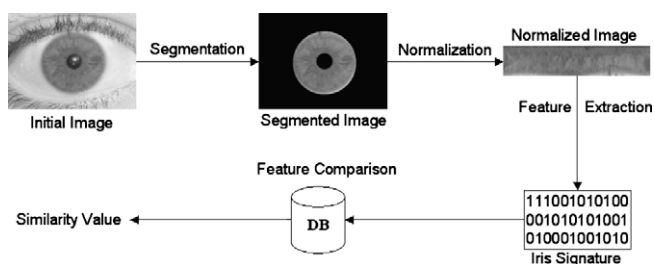


Fig. 1. Typical stages of published iris recognition methods.

proposed the use of an integro-differential operator to find both the iris inner and outer borders. This operator remains up-to-date and was proposed with some minor differences in 2004, by Nishino and Nayar [11]. Similarly, Camus and Wildes [12] and Martin-Roche et al. [13] used integro-differential operators that search over tridimensional spaces, having as goal the maximization of equations that localize both iris borders.

Wildes [1] started the segmentation of the iris ring by the construction of a binary edge-map. Next, used the circular Hough transform to fit circles that delimit the iris ring. This is the most usually seen method in the iris segmentation literature and is proposed with minor variants by Wang and co-workers [14,15,2]. Also based in Wildes', Proença and Alexandre proposed a method [16] that uses a clustering process to increase the robustness to noisy data.

The method proposed by Du et al. [18] is based on the previous detection of the pupil. The image is then transformed into polar coordinates and the iris outer border localized as the largest horizontal edge resultant from Sobel filtering. This approach may fail in case of non-concentric iris and pupil, and of very dark iris textures.

Morphologic operators were applied by Mira and Mayer [19] to find both iris borders. They detected the inner border by sequentially using threshold, image opening and closing techniques. The outer border was similarly detected.

Based on the assumption that the intensity values of close-up iris images can be well represented by a mixture of three Gaussian distributions, Kim et al. [20] proposed the use of the Expectation Maximization algorithm to estimate the parameters of the respective distributions. They expect that 'Dark', 'Intermediate' and 'Bright' distributions respectively contain the pixels corresponding to the pupil, iris and reflections areas.

## 3. Experiments

In this section we describe the types of segmentation errors used in our experiments and analyze their impact on the recognition error rates.

The Wildes' [1] method was used to segment all the iris images. In order to enable the experiments, we manually verified that the algorithm has accurately localized all the pupillary and scleric iris borders.

The cartesian to polar transformation was made through the widely used "Daugman Rubber Sheet" [7], yielding dimensionless polar representations of the irises with dimensions of 512 (width) by 64 (height) pixels.

Three distinct feature extraction methods were implemented [8,9,2]. As common points, they share the analysis of the normalized (polar) iris representation, the extraction of binary signature components and the use of the Hamming distance to compute the dissimilarity between signatures. Daugman [8] convolved the normalized iris data with a bank of Gabor filters at different resolutions and orientations to extract the biometric signature. Ali and Hassanien [9] encoded the iris data through the dyadic wavelet decomposition (using the Haar as mother wavelet), being this approach one of the most frequently seen in the iris recognition literature. Finally, Ma et al. [2] were also based in the dyadic wavelet decomposition to build a set of binary sequences that localize regions of the iris with high intensity variations.

### 3.1. Experiments databases

There are presently seven public and freely available iris image databases for biometric purposes: Chinese Academy of Sciences [5] (CASIA, three distinct versions), Multimedia University (MMU, two versions), University of Bath (BATH), Palacký University Olomouc

(UPOL), Iris Challenge Evaluation [6] (ICE), West Virginia University (WVU) and University of Beira Interior [4] (UBIRIS, two versions).

CASIA database contains near infra-red (NIR) images and is by far the most widely used on iris biometric experiments, having presently three distinct versions. Its images incorporate few types of noise, almost exclusively related with eyelid and eyelash obstructions, similarly to the images of the MMU and BATH databases. UPOL images were captured with an optometric framework, obtaining optimal images with extremely similar characteristics. Although ICE and WVU are NIR databases that contain more heterogeneous images, their lack of images with significant reflections occluding the iris rings constitutes a weak point, regarding the simulation of less constrained imaging conditions. Oppositely, images of the UBIRIS database were captured on the visible wavelength, under natural lighting and heterogenous imaging conditions, which explains their higher heterogeneity.

According to the aforementioned discussion, we selected 10 images per subject from three databases (Fig. 2): UBIRIS (first and second version), CASIA (third version) and ICE databases, giving a total of 5000 images. Further, we extracted the biometric signatures from these images (using the afore described feature extraction strategies) and compared each signature with all the remaining ones of the respective data set, performing a total of respectively 22,500 and 4,475,000 intra- and inter-class comparisons.

Images of the UBIRIS databases have fixed dimensions of 400 (width) by 300 (height) pixels and horizontal and vertical resolution of 300 dpi. The irises have radius values between 80 and 100 pixels and the pupils values between 15 and 35 pixels. Images of the CASIA database have  $320 \times 280$  pixels and horizontal and vertical resolution of 96 dpi. The irises have radius values between 87 and 110 and the pupils between 20 and 45 pixels. Finally, images of the ICE database have  $320 \times 240$  pixels with vertical and horizontal resolution of 96 dpi. The irises have radius values between 73 and 97 pixels and the pupils between 13 and 38 pixels.

### 3.2. Types of segmentation errors

The iris segmentation method used in our experiments approximates both the iris and the pupil as circles. Thus, each border can be defined by its center coordinates  $(x, y)$  and radius  $r$ . Let  $(x_s, y_s)$

and  $r_s$  be respectively the center coordinates and radius of the circle resultant of the segmentation process. Also, let  $(x_t, y_t)$  and  $r_t$  be the respective parameters of the true iris circle.

In our implementation of the segmentation method we artificially simulated two types of errors:

- **Translational errors:** we defined a translational error of  $p$  pixels when  $\|x_s - x_t\| + \|y_s - y_t\| = p$ . It occurs when the center of the segmented circle is deviated  $p$  pixels from the center of the true circle. Fig. 3b gives an example of a translational error in the segmentation of the pupillary border.
- **Scale errors:** as Fig. 3c and d illustrate, a scale error occurs when the detected and the true circles have different radius values. If  $\|r_s - r_t\| = p$  then we considered this as a scale error of  $p$  pixels.

These two types of errors on each iris border enabled the appearance of four distinct segmentation errors: translational error on the scleric border, translational error on the pupillary border, scale error on the scleric border and scale error on the pupillary border. Other types of segmentation errors can be expressed as linear combinations of the above described errors and were not the subject of our analysis.

### 4. Results and discussion

By using Hamming distance as the dissimilarity measure, each comparison between iris signatures gives a value, closed in the  $[0, 1]$  interval, that is directly proportional to the dissimilarity between the compared irises.

On each test, we made all the possible intra- and inter-class comparisons between signatures extracted from the respective data set. Table 1 contains the average separability between the intra- and inter-class comparisons and the obtained error rates, regarding the accuracy of the segmentation stage. “ $FRR_{FAR=0}$ ” corresponds to the false rejection rates when the false acceptances were minimized, “EER” gives the approximated equal error rates and the last columns contain the value of a Fisher-ratio test (FR) given by:

$$FR = \frac{(\mu_E - \mu_I)^2}{\sigma_I^2 + \sigma_E^2} \quad (1)$$

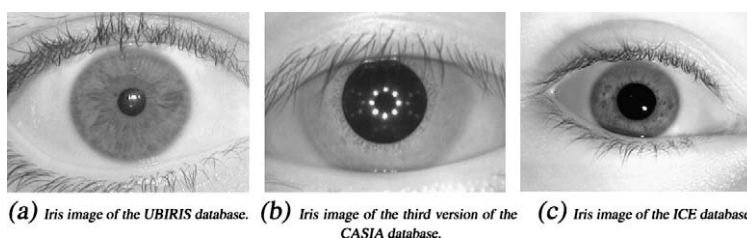


Fig. 2. Examples of close-up iris images of the databases used in our experiments: (a) UBIRIS, (b) third version of CASIA and (c) ICE.

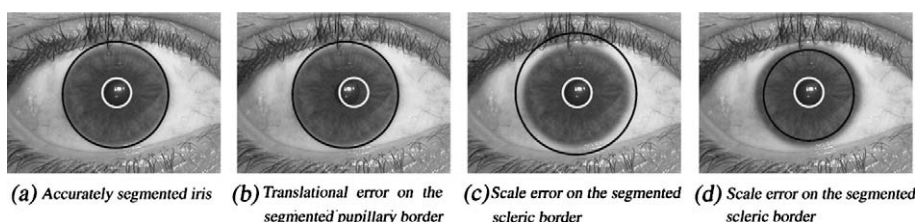


Fig. 3. Accurate and inaccurately segmented iris images.

**Table 1**

Separability between the intra- and inter-class comparisons and respective obtained recognition error rates, regarding the accuracy of the segmentation stage.  $FRR_{FAR=0}$  gives the false rejection rates with no false acceptances, EER corresponds to the approximated equal error rates and Fisher-ratio test gives the values obtained by (1).

Error	FRR <sub>FAR=0</sub> (%)			EER (%)			Fisher-ratio test		
	CASIA	ICE	UBIRIS	CASIA	ICE	UBIRIS	CASIA	ICE	UBIRIS
No error	6.81	9.90	12.12	1.31	2.63	4.27	22.75	20.95	17.54
<i>Translational error on the pupillary border</i>									
1 pixel	7.96	11.49	15.80	1.85	3.69	5.48	20.31	18.71	16.95
2 pixel	12.15	15.76	18.91	2.98	4.48	6.44	18.56	16.94	15.60
3 pixels	15.97	17.06	21.42	3.90	5.11	7.84	17.64	14.75	14.67
4 pixels	18.95	20.42	26.15	4.95	6.97	8.34	15.63	13.47	13.16
5 pixels	21.48	24.54	30.70	5.58	8.53	10.50	14.70	12.27	11.97
<i>Translational error on the scleric border</i>									
1 pixel	7.69	10.09	13.93	1.81	3.66	5.29	19.83	18.91	16.72
2 pixels	12.91	13.72	17.77	2.99	4.19	7.12	17.08	17.72	15.27
3 pixels	15.89	18.13	21.59	3.92	5.25	8.81	15.58	15.28	13.75
4 pixels	19.09	21.25	24.66	5.00	7.11	8.75	14.53	13.58	12.71
5 pixels	21.72	24.84	29.93	5.68	8.38	10.02	14.03	12.97	11.72
<i>Scale error on the pupillary border</i>									
1 pixel	7.07	9.93	12.99	1.33	3.16	5.31	20.68	18.90	16.84
2 pixels	7.59	10.08	13.12	1.61	3.22	5.51	19.92	18.08	15.98
3 pixels	8.05	10.77	13.56	1.71	3.79	5.85	18.74	17.91	15.28
4 pixels	8.40	11.40	13.88	1.79	4.43	6.85	18.45	16.82	14.43
5 pixels	9.53	11.93	14.46	1.95	5.06	7.26	17.22	15.83	13.93
<i>Scale error on the scleric border</i>									
1 pixel	6.99	9.61	13.11	1.37	3.26	5.35	20.69	18.92	16.89
2 pixels	7.61	10.07	13.47	1.45	3.90	5.70	20.12	17.71	16.02
3 pixels	8.07	10.73	13.80	1.50	4.28	6.44	19.37	17.10	15.49
4 pixels	8.67	11.00	14.07	1.77	4.91	7.01	18.80	16.29	14.21
5 pixels	9.49	11.86	14.80	1.99	5.12	7.39	17.80	15.63	13.98

where  $\mu_I$  and  $\mu_E$  respectively indicate the mean of the intra- and inter-class comparisons.  $\sigma_I$  and  $\sigma_E$  indicate the respective standard deviations.

Not surprisingly, the highest separability between the intra- and inter-class comparisons was obtained with accurate segmentation. Also, we observed that translational segmentation errors have a stronger impact in the recognition error rates than scale errors do, which is explained by the fact that this type of errors corresponds to errors in phase, causing many bits to appear flipped in the iris signatures and corrupting the comparison between signatures.

When comparing the impact on the error rates caused by segmentation errors on each iris border, we obtained very close results, which we justify by the iris normalization process and by the fact that we did not privileged specific iris regions in the feature extraction process.

At first, the transformation into the pseudo-polar coordinate system is defined as a linear combination of both borders. Thus, they should naturally play similar roles in the process and similarly affect the error rates.

Finally, it is often considered that errors in the segmentation of the pupillary border are of bigger concern, regarding the recognition error rates. It is suspected that deployed systems privilege the inner regions of the iris to encode the iris signature, which explains their higher tolerance to errors in the segmentation of the scleric border. As our purpose was not to specifically evaluate one recognition method, we did not privileged any iris region in the feature extraction stage, which justifies that errors in the segmentation of the pupillary and scleric iris borders tend to similarly deteriorate the recognition results.

Fig. 4 stresses the above described increase of the error rates. It contains the DET curves obtained with accurate segmentation (continuous lines) and translational errors in the pupillary border of respectively one (dashed lines) and three pixels (dotted lines). Confirming our previous observations, a significant increase in the error rates has occurred, which has evident proportionality to the amplitude of the segmentation error. Also, we observed that this deterioration was similarly observed either in the less noisy (CASIA and ICE) and noisiest (UBIRIS) data sets.

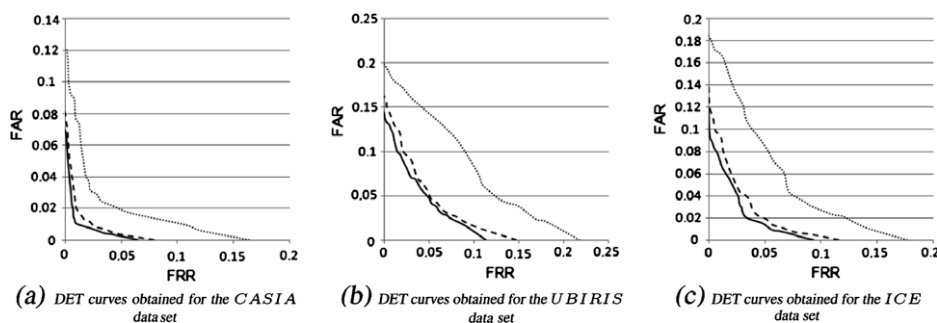


**Fig. 4.** Comparison between the Detection Error Tradeoff (DET) obtained with accurate (continuous lines) and inaccurate iris segmentation. The inaccuracies correspond to translational errors on the pupillary border of one (dashed lines) and three pixels (dotted lines).

## 5. Conclusions

In this paper we analyzed the major role of the iris segmentation stage in the error rates of three typical iris recognition methods.

We used three data sets from widely used iris databases (third version of CASIA, first and second version of UBIRIS and ICE) to analyze the increase of the error rates when the iris is inaccurately segmented. Having defined four types of segmentation errors (translational and scale errors on the iris inner and outer borders), we observed the most significant increment in the error rates when translational errors occur, which can be explained by the fact that this type of errors corresponds to errors in phase and make components of the biometric signature to appear flipped.

According to these results, the development of methods to detect inaccurately segmented irises should be relevant, essentially to avoid the prosecution of the recognition processes to later stages.

Finally, we observed that the increment in the error rates is directly proportional to the amplitude of the segmentation inaccuracies, either in the highly noisy database of visible wavelength images (UBIRIS) and the less noisy iris databases of near infrared images (CASIA and ICE).

## Acknowledgements

We acknowledge the financial support given by “FCT-Fundação para a Ciência e Tecnologia” and “FEDER” in the scope of the PTDC/EIA/69106/2006 research project “BIOREC: Non-Cooperative Biometric Recognition”.

## References

- [1] R.P. Wildes, Iris recognition: an emerging biometric technology, in: *Proceedings of the IEEE*, vol. 85, no. 9, USA, September 1997, pp. 1348–1363.
- [2] L. Ma, Y. Wang, D. Zhang, Efficient iris recognition by characterizing key local variations, *IEEE Transactions on Image Processing* 13 (6) (2004) 739–750, June.
- [3] M. Vatsa, R. Singh, A. Noore, Reducing the false rejection rate of iris recognition using textural and topological features, *International Journal of Signal Processing* 2 (1) (2005) 66–72.
- [4] H. Proença, L.A. Alexandre, UBIRIS: a noisy iris image database, in: *13th International Conference on Image Analysis and Processing (ICIAP2005)*, September 2005, pp. 970–977. Available from: <<http://iris.di.ubi.pt>>.
- [5] Institute of Automation, Chinese Academy of Sciences, CASIA iris image database, 2004. Available from: <<http://www.sinobiometrics.com>>.
- [6] National Institute of Standards and Technology, Iris Challenge Evaluation, 2006. Available from: <<http://iris.nist.gov/ICE/>>.
- [7] J.G. Daugman, High confidence visual recognition of persons by a test of statistical independence, *IEEE Transactions on Pattern Analysis and Machine Intelligence* 25 (11) (1993) 1148–1161.
- [8] J.G. Daugman, How iris recognition works, *IEEE Transactions on Circuits and Systems for Video Technology* 14 (1) (2004) 21–30.
- [9] J. Ali, A. Hassanien, An iris recognition system to enhance e-security environment based on wavelet theory, *AMO – Advanced Modeling and Optimization* 6 (2) (2003) 93–104.
- [10] W.W. Boles, B. Boashash, A human identification technique using images of the iris and wavelet transform, *IEEE Transactions on Signal Processing* 46 (4) (1998) 1185–1188.
- [11] K. Nishino, S.K. Nayar, Eyes for relighting, *ACM Transactions on Graphics* 23 (3) (2004) 704–711.
- [12] T. Camus, R. Wildes, Reliable and fast eye finding in close-up images, in: *Proceedings of the IEEE 16th International Conference on Pattern Recognition*, 2002, pp. 389–394.
- [13] D. Martin-Roche, C. Sanchez-Avila, R. Sanchez-Reillo, Iris recognition for biometric identification using dyadic wavelet transform zero-crossing, *IEEE Aerospace and Electronic Systems Magazine* 17 (10) (2002) 3–6.
- [14] J. Huang, Y. Wang, T. Tan, J. Cui, A new iris segmentation method for recognition, in: *Proceedings of the 17th International Conference on Pattern Recognition (ICPR04)*, vol. 3, 2004, pp. 23–26.
- [15] L. Ma, Y. Wang, T. Tan, Iris recognition using circular symmetric filters, in: *Proceedings of the 25th International Conference on Pattern Recognition (ICPR02)*, vol. 2, 2002, pp. 414–417.
- [16] H. Proença, L.A. Alexandre, Iris segmentation methodology for non-cooperative iris recognition, *IEE Proceedings – Vision Image and Signal Processing* 153 (2) (2006) 199–205.
- [17] H. Proença, L.A. Alexandre, The NICE. I – noisy iris challenge evaluation. Part I, in: *Proceedings of the First International Conference on Biometrics: Theory, Applications and Systems (BTAS07)*, 2007, pp. 414–417.
- [18] Y. Du, R. Ives, D. Etter, T. Welch, C. Chang, A new approach to iris pattern recognition, in: *Proceedings of the SPIE European Symposium on Optics/Photonics in Defence and Security*, vol. 5612, October 2004, pp. 104–116.
- [19] J. Mira, J. Mayer, Image feature extraction for application of biometric identification of iris – a morphological approach, in: *Proceedings of the 16th Brazilian Symposium on Computer Graphics and Image Processing (SIBGRAPI 2003)*, Brazil, October 2003, pp. 391–398.
- [20] J. Kim, S. Cho, J. Choi, Iris recognition using wavelet features, *Journal of VLSI Signal Processing*, vol. 38, Kluwer Academic Publishers, 2004. pp. 147–256.